eIF4G-driven translation initiation of downstream ORFs in mammalian cells

Risa Nobuta[1], Kodai Machida[2], Misaki Sato[1], Satoshi Hashimoto[1], Yasuhito Toriumi[1], Shizuka Nakajima[1], Daiki Suto[1], Hiroaki Imataka[2,*] and Toshifumi Inada [1,*]

[1]Graduate School of Pharmaceutical Sciences, Tohoku University, Sendai 980-8578, Japan and [2]Department of Applied Chemistry, Graduate School of Engineering, University of Hyogo, Himeji 671-2280, Japan

ABSTRACT

Comprehensive genome-wide analysis has revealed the presence of translational elements in the 3′ untranslated regions (UTRs) of human transcripts. However, the mechanisms by which translation is initiated in 3′ UTRs and the physiological function of their products remain unclear. This study showed that eIF4G drives the translation of various downstream open reading frames (dORFs) in 3′ UTRs. The 3′ UTR of *GCH1*, which encodes GTP cyclohydrolase 1, contains an internal ribosome entry site (IRES) that initiates the translation of dORFs. An *in vitro* reconstituted translation system showed that the IRES in the 3′ UTR of *GCH1* required eIF4G and conventional translation initiation factors, except eIF4E, for AUG-initiated translation of dORFs. The 3′ UTR of *GCH1*-mediated translation was resistant to the mTOR inhibitor Torin 1, which inhibits cap-dependent initiation by increasing eIF4E-unbound eIF4G. eIF4G was also required for the activity of various elements, including polyU and poliovirus type 2, a short element thought to recruit ribosomes by base-pairing with 18S rRNA. These findings indicate that eIF4G mediates translation initiation of various ORFs in mammalian cells, suggesting that the 3′ UTRs of mRNAs may encode various products.

INTRODUCTION

Thousands of different mRNAs simultaneously access a pool of ribosomes for protein expression in mammalian cells. The recruitment of the ribosome to a specific mRNA is a critical step in the production of proteins in cells. In eukaryotes, protein-coding messenger RNAs (mRNAs) are modified with a 5′ cap and a 3′ poly(A) tail, with both being crucial for canonical initiation of translation. The crucial step in the initiation of translation is the assembly of competent ribosomes at appropriate initiation sites at the 5′ termini of open reading frames (ORFs) of mRNAs (1). Ribosomes recognize initiation codons primarily by the 5′-end dependent 'scanning' pathway, which is mediated primary by the interaction of the eIF4F complex with the cap portion of the eIF4F complex. The standard mode of the scanning pathway in eukaryotes is initiated by the binding of the translation initiation factor eIF4F to the cap at the 5′ end of mRNA. eIF4F consists of a scaffold protein eIF4G, which interacts with the cap-binding subunit eIF4E, the helicase eIF4A, eIF3 and polyadenylate-binding protein (PABP). eIF4G recruits the 43S preinitiation complex (PIC), composed of a 40S subunit loaded with eIF1, eIF1A, eIF3, eIF5 and the ternary complex eIF2-Met-tRNA$_i^{Met}$-GTP. The 43S PIC machinery moves in the 3′ direction to detect the initiation codon, with the helicase eIF4A resolving any encountered elements of secondary structure. Once the initiation codon is located, it is bound by the anticodon on the initiator tRNA. eIF2-bound GTP hydrolysis triggers the removal of the eIFs from the 40S subunit, with eIF5B assisting the joining of the 60S ribosomal subunit to the 40S subunit to form the 80S ribosome initiation complex (1).

In addition to conventional cap-dependent translation, an alternative mode of translation initiation depends on the specific cis-acting RNA sequence internal ribosome entry site (IRES) (2). The IRES is usually upstream of the start codon of each mRNA, and drives the internal initiation pathway in a manner that is cap- and end-independent, but is dependent on a limited subset of initiation factors. The cap-independent translation from IRES is essential for the synthesis of many human and viral proteins. Because their genomes have limited coding capacity, viruses have evolved various ways to hijack critical steps in the cellular gene expression pathway, with IRES-mediated initiation of translation being critical for viral propagation (3). Some viruses express a protease that cleaves the initiation factor eIF4G, a component of the cap-binding complex, blocking cap-dependent initiation of translation and resulting in a shutdown of translation in infected cells. The translational ma-

---

chinery is, thus, fully available for the viral mRNA, with translation of viral mRNA occurring in a cap-independent manner. Virus IRESs form complicated secondary or tertiary structures assembled with stem-loops and pseudo-knots, and act as ribosome landing pads through multiple RNA–RNA and RNA–protein interactions (4–6).

Since IRES was first shown to be involved in the translation of picornavirus RNA, as an alternative to the eukaryotic 'scanning model', IRES has been found to be the major translation initiation pathway for several families of viruses. IRESs are highly diverse in structure and mechanism, underscored by varying requirements for canonical initiation factors or specific stimulatory IRES *trans*-acting factors (ITAFs). Importantly, viral infection by several mechanisms inhibits translation initiation in host cells (7). During virus infection, translation factors, such as eIF4G, eIF4A and PABP, are cleaved by viral proteases (8–10), whereas others, such as eIF4E, are inactivated (11). In addition, hepatitis C virus (HCV) and cricket paralysis virus (CrPV) have been shown to activate the RNA-dependent protein kinase PKR, which inactivates eIF2 by phosphorylation in a cell-specific manner (12,13). Cellular protein synthesis is down-regulated by the limited availability of initiation factors, enhancing the expression of viral proteins and viral replication while suppressing the expression of cellular proteins (14–16). IRES are crucial for the virus to take over the eukaryotic translation machinery and efficiently suppress the translation of standard mRNAs in infected cells.

A subset of cellular mRNAs, with long and highly structured 5′-UTRs, was found to have putative IRES activity and to act as a template for protein synthesis under limited conditions. IRES-mediated translation initiation is involved in various biological functions, including the response of cells to environmental stresses, such as nutrient deprivation, endoplasmic reticulum (ER) stress and hypoxia (17–19). Recent technological advances have allowed the identification and quantitation of proteins produced in cells by ribosome profiling. RNA elements have been shown to facilitate the 5′-end-independent initiation of translation in human transcripts and the polyprotein regions of uncapped RNA viruses (20). Potential IRES elements have been identified in 10% of randomly selected human 5′ UTRs and even in 3′ UTRs (20). These potential IRES elements can be classified into three *cis*-regulatory elements: complex global RNA folds, polyU and poliovirus type 2 (PV2) short IRES elements, and short sequence elements that recruit ribosomes for internal initiation by base-pairing with 18S rRNA. To date, however, these findings have not been confirmed functionally or biochemically (2,21–22), nor have these IRESs in cellular mRNAs been shown to mediate protein synthesis.

This study was performed to identify the elements in 3′ UTRs that initiate the translation of downstream ORFs (dORFs). *Cis*-elements in the 3′ UTR of *GCH1*, the gene encoding GTP cyclohydrolase 1, were found to function as IRESs to initiate translation of dORFs. An *in vitro* reconstituted translation system showed that the IRES in the 3′ UTR of *GCH1* required eIF4G and conventional translation initiation factors, except eIF4E, for AUG-initiated translation of dORFs. 3′ UTR-mediated translation was resistant to the mTOR inhibitor Torin 1, which increases the

level of eIF4E-unbound eIF4G. These findings demonstrate that eIF4G drives the translation of dORFs in the 3′ UTRs of mammalian cells, suggesting that the 3′ UTR of mRNAs encode various products.

MATERIALS AND METHODS

Plasmid constructs

All recombinant DNA techniques were performed according to standard procedures using *Escherichia coli* DH5α for cloning and plasmid propagation. Site-directed mutagenesis was performed by overlap-extension polymerase chain reaction (PCR). All cloned DNA fragments generated by PCR amplification were verified by sequencing. Plasmids and oligonucleotides used in this study are listed in Supplementary Tables S1 and 2, respectively.

To construct V5-Rluc-dORF-Fluc-HA, DNA fragments encoding firefly luciferase (Fluc) and Renilla luciferase (Rluc) were PCR amplified from phRL-cmv and phFL-cmv (Promega) plasmids, respectively, and inserted downstream of the CMV promoter between the NheI and XhoI sites in pcDNA3.1 (+). The DNA sequences to measure translation arrest were amplified by PCR or generated by annealing two oligonucleotides, and inserted between the HindIII and NotI sites in the dORF region. The inserted sequences are listed in Supplementary Table S1 (23,24).

To construct V5-Rluc-stop-dORF-Fluc-HA, a DNA fragment encoding the Rluc protein was amplified by PCR from the plasmid V5-Rluc-dORF-Fluc-HA using the primers OIT 4242 (5′- TAGATGGCTAGCATGGGTAA GCCTATCCCTAACCCTCTCCTCGGTCTCGATTCT ACGACTTCGAAAGTTTATGATCC-5′) and OIT 4225 (5′-GAATTCAAGCTTTCATTGTTCATTTTTGAGAA CTC-3′), and was inserted into the NheI and HindIII sites in V5-Rluc-dORF-Fluc-HA. The DNA sequences to measure IRES activities were amplified by PCR or generated by annealing two oligonucleotides, and were inserted between the HindIII and NotI sites in the dORF region. Inserted sequences are listed in Supplementary Table S1.

To construct SL-V5-Rluc-dORF Fluc-HA and SL-V5-Rluc-stop-dORF-Fluc-HA, a DNA fragment encoding a stem-loop structure was generated by annealing two oligonucleotides and was inserted between the KpnI sites upstream of V5-Rluc-dORF-Fluc-HA and V5-Rluc-stop-dORF-Fluc-HA, respectively. To construct pBluescript II (SK⁺)V5-Rluc-stop-dORF-Nluc-HA, fragments encoding V5-Rluc and Nano Luc (Nluc) were amplified by PCR from V5-Rluc-stop-dORF-Fluc-HA and pNL1.1.cmv (Promega), respectively, and inserted between the KpnI and XbaI sites in pBluescript II (SK⁺), yielding clones containing the expected 3′ ends followed by poly(A) tails. To construct CMV(-)dORF-Fluc-HA, a fragment encoding dORF-Fluc-HA was amplified by PCR from V5-Rluc-stop-dORF-Fluc-HA, and was inserted between the NluI and XhoI sites in pcDNA3.1(+).

For *in vitro* transcription template DNA, V5-Rluc-stop (TGA or TAA)-dORF-Nluc-HA was digested with KpnI and XbaI, and cloned into the pBluescript II SK+ vector.

Cell culture and treatments

HEK293T and N2A cells were cultured in Dulbecco's modified Eagle's medium with 10% fetal bovine serum and penicillin/streptomycin. HEK293T and N2A cells were transfected with 2 μg plasmid DNA with PEI MAX. Briefly, 12 μl PEI MAX was added to 150 μl Opti-mem with DNA, mixed and pipetted into each well of a 12-well plate containing 4×10^5 cells. The medium was replaced 4 h later, and the cells were harvested after 24 h. Cells transfected with dual luciferase reporter plasmids were treated 20 h after transfection with 25, 50, 100 or 250 nM Torin1 for 4 h.

In vivo luciferase reporter assay

In vivo luciferase reporter assays were performed using Nano-Glo and Renilla Luciferase Assay Systems (Promega, Madison, WI, USA). Cells were harvested and lysates were prepared with 50–100 μl Passive Lysis Buffer (Promega) and incubated for 20 min at room temperature. Protein concentrations were determined using the Bradford assay (Bio-Rad, Hercules, CA, USA).

Electrophoresis and western blotting

Protein samples were separated on 10% polyacrylamide/sodium dodecyl sulphate gels and transferred to nitrocellulose membranes, which were blocked by incubation with 5% skim milk in PBST (10 mM Na_2HPO_4/NaH_2PO_4, pH 7.5; 0.9% NaCl; 0.1% Tween-20). The membranes were hybridized with the primary antibodies listed in Supplementary Table S3. The membranes were washed three times with PBST and incubated with secondary antibodies conjugated to horseradish peroxidase. After three additional washes with PBST, chemiluminescence was detected by ImageQuant LAS4000 (Chicago, Illinois, GE Healthcare).

In vitro translation with the reconstituted system

mRNAs were transcribed *in vitro* in the presence of either ^{7}mGpppG or ApppG (for V5-Rluc-stop-dORF-Nluc-HA mRNA). To reconstitute translation, eIF1 (0.96 μM), eIF1A (0.96 μM), eIF2 (0.96 μM), eIF2B (0.04 μM), eIF3 (0.04 μM), eIF4A (2.40 μM), eIF4B (0.48 μM), eIF4G and eIF4E (0.16 μM), eIF5 (0.32 μM), eIF5B (0.16 μM), PABP (3.84 μM), DHX29 (0.08 μM), pure-tRNA (1 μg/μl), eEF1s (50 μM), 40S ribosomal subunit (0.48 μM), 60S ribosomal subunit (0.48 μM), eEF2 (0.96 μM), eRF1/3 (50 ng/μl), AA mix (0.1 mM), ARS mix (150 ng/μl), PPA1 (0.1 μM) and ABCE1 (0.48 μM) were mixed with 0.5 μl reporter mRNA (150 ng/μl), and the mixture (2.52 μl) was incubated for up to 2 h at 32°C. The reaction was stopped by immersion in liquid N_2, and Nano-Glo and Renilla luciferase activities were measured. The recombinant proteins translated *in vitro* are listed in Supplementary Table S4.

Toeprinting of 48S initiation complex with the reconstituted translation factors

RNA–protein complex was formed by incubating initiation factors and reporter mRNA (100 ng) transcripts for 10 min at 32°C in buffer (100 mM KCl, 20 mM Hepes-KOH [pH 7.5]). Each reaction mixture contained 0.96 μM eIF1, 0.96 μM eIF1A, 0.96 μM eIF2, 0.04 μM eIF3, 2.4 μM eIF4A, 0.48 μM eIF4B, 0.16 μM eIF4G$^{84–1599}$, and 0.1 mM amino acid mix (1 μg/μl each), in the absence/presence of 40S subunits. Incubation was continued for 3 min at 32°C following the addition of 2 pmol of 5′ IRDye700-labeled primer 5′-AGATTCTGAAACAAACTGGACACACCT-3′ (complementary to Nano Luc nt 81–107). The reaction mixtures were placed on ice and incubated for 45 min at 32°C in a 20 μl reaction volume that contained RT mix (8 mM Mg(AOc)$_2$, 0.5 mM dNTPs, 8.6 μl buffer A (2 mM DTT, 100 mM KOAc, 20 mM Tris [pH 7.5], 2.5 mM Mg(AOc)$_2$, 1 mM adenosine triphosphate (ATP), 0.1 mM GMP-PNP, 0.25 mM spermidine) and 10U of AMV reverse transcriptase (Promega, 10 U/μl), followed by extraction with phenol–chloroform and ethanol precipitation. Each cDNA pellet was dissolved in 5 μl deionized formamide with 5 mg/ml blue dextran. The cDNA was linearized at 95°C for 5 min followed by incubation on ice for 5 min and resolution on 5% polyacrylamide-TBE-urea sequencing gels by electrophoresis at 1000 V for 120 min. The fluorescence of IRDye700 was detected by FLA-9000 (Fujifilm). The size of each cDNA was determined by comparison with a sequencing ladder of corresponding reporter plasmids or PCR fragment DNAs prepared using the same primers and a Thermo Sequenase Cycle Sequencing Kit (USB Cat#78500 1 KT).

Toeprinting of the 80S initiation complex with Rabbit Reticulocyte Lysate (RRL)

The translation initiation complexes were assembled in RRL (RRL; Flexi RRL system; Promega; 2.6 mM endogenous Mg^{2+}) in the presence of 20 μM amino acid mixture, 70 mM KOAc, 3 μl RRL, 4 U RNasin Plus RNase Inhibitor (Promega) and DEPC treated water or 1 μl of a water solution of cycloheximide (10 mg/ml). The mixtures, in a final volume of 4.32 μl, were preincubated for 5 min at 32°C, incubated for an additional 10 min at 32°C after the addition of reporter mRNA (100 ng) and incubated for 3 min further at 32°C following the addition of 2 pmol of 5′ IRDye700-labeled primer (see above). Toeprint analysis was performed as described above.

Primer extension to determine the 5′ end of the truncated Fluc mRNA

A total of 7.5 μg of RNA was subjected to reverse transcription (RT) by using SuperScript IIIReverse Transcriptase (invitrogen Cat# 18080044) with 5′-IRDye700-labeled primer (IDT) complementary to *FLUC* nucleotide sequence (5′-GTGATGTTCACCTCGATATGTGCAT-3′). Equal amount of chloroform was added to the reaction and it was mixed by vortex. Water layer was collected after centrifuge, followed by ethanol precipitation with one-tenth amount of 5 M NH$_4$OAc, twice and half amount of ethanol and 1 μl of glycogen. Obtained cDNA pellet was dissolved in 5μl of deionized formamide with 5 mg/ml blue dextran (SIGMA, #D4772). cDNA Sample was linearized at 70°C for 2 min followed by on ice for 5 min, and resolved on 5% polyacrylamide-TBE-7Murea sequencing gel

by electrophoresis at 1000 V for 180 min. Fluorescence of IRDye700 was detected by FLA-9000 (Fujifilm). The size of the RT product was determined compared to a sequencing ladder of corresponding reporter plasmid DNA prepared by using same primer and Thermo Sequenase Cycle Sequencing Kit (USB Cat# 78500 1 KT).

Quantification and statistical analysis

All quantitative data are presented as the mean ± standard deviation (S.D.) from at least three independent experiments. IRES activities were quantified by measuring normalizing luciferase activity to Renilla activity for three separate experiments, with error bars representing S.D.

RESULTS

Dual reporter system identification of elements in 3′ UTRs that initiate translation of dORFs

Comprehensive genome-wide analysis has revealed the presence of many translational elements in the 3′ UTRs of human transcripts (20). The present study was performed to semi-comprehensively analyze the initiation of translation in the 3′ UTRs of genes in which readthrough mutations (stop codons mutated to sense codons) are responsible for diseases (24). Initiation of translation was monitored by constructing 80 reporters, in which the 3′ UTR between a stop codon of the main ORF and the next in-frame stop codon of each gene was inserted between the ORFs for Renilla luciferase (Rluc) and firefly luciferase (Fluc) (Figure 1A). In these reporters, the Rluc ORF has no termination codon, and the Fluc ORF has no AUG initiation codon. These dual reporters, *V5-Rluc(noSTOP)-X-(noAUG)FLuc*, were utilized to identify the putative IRES activity that initiates translation of dORFs in the 3′ UTRs. The various dual reporters were transfected into human HEK293 cells. More than half the sequences repressed the expression of downstream Fluc activity (Supplementary Figure S1), findings consistent with translation arrest evaluated with the *GFP-E2A-X-E2A-RFP* reporter system (23). The ratio of luciferase activities of the reporters with 20 elements was >100% (Supplementary Figure S1), and that of the reporters with four 3′ UTRs, *CRYBB1*, *PEX1*, *SH2D1A* and *GCH1*, was >200% (Figure 1B). Western blot analysis showed Fluc products derived from *V5-Rluc(noSTOP)-X-(noAUG)Fluc-HA* reporters, into which four 3′ UTRs and sequences encoding full-length V5-Rluc-X-FLuc-HA fusion proteins had been inserted (Figure 1C). Cryptic promoter activity may initiate transcription from these elements, resulting in the production of Fluc. To validate the promoter activity of these elements, the CMV promoter of pcDNA3.1(+) was replaced with these elements as well as HCV and the Fluc activity dependent on promoter activity was measured. Insertion of these elements resulted in little or no residual Fluc activity (Supplementary Figure S2). A comparison with the relatively high expression of Fluc from *V5-Rluc(noSTOP)-X-(noAUG)Fluc-HA* reporters by these elements suggested that the promoter activity of these elements did not account for the expression

of downstream Fluc from the dual reporter construct. Alternatively, these Fluc products may have been produced by the initiation of translation from these elements in the 3′ UTRs or by the cleavage of full-length Rluc-X-Fluc protein. To determine whether the Fluc products were produced by cleavage of full-length Rluc-X-Fluc protein, a termination codon was inserted just after the upstream Rluc (Figure 1D). Western blot analysis detected the V5-Fluc products derived from *V5-Rluc(Stop)-X-(noAUG)FLuc-HA* dual reporters that contain a termination codon of *Rluc* (Figure 1E, even lanes), indicating that the full-length Rluc-X-Fluc is not a precursor of the V5-Fluc products. Western blot analysis detected the middle bands derived from *V5-Rluc(noSTOP)-PEX1-(noAUG)Fluc-HA* and *V5-Rluc(noSTOP)-GCH1-(noAUG)Fluc-HA* (Figure 1C, lanes 3 and 5). The introduction of a termination codon (STOP) at the 3' end of Rluc ORF eliminated middle bands derived from *V5-Rluc(noSTOP)-PEX1-(noAUG)Fluc-HA* (Figure 1E, lanes 5–6) but not *V5-Rluc(noSTOP)-GCH1-(noAUG)Fluc-HA* (Figure 1E, lanes 9–10), indicating that the two bands derived from *V5-Rluc(noSTOP)-GCH1-(noAUG)Fluc-HA* are translated from the 3′ UTR of *GCH1*. The luciferase assays revealed that the levels of Rluc were reduced when Fluc was translated from three 3′ UTRs, *CRYBB1*, *PEX1* and *SH2D1A* (Figure 1F, right panel). These results strongly suggest that these regions have both initiation codons and activities enabling translation from these codons. The translation of dORFs repressed the translation of upstream ORFs, suggesting that dORF products regulate the translation of main ORFs.

Initiation codons for dORF translation in 3′ UTR elements

To identify the minimal regions of these 3′ UTRs required to translate *(no-AUG)Fluc*, deletion analysis was performed with various deletion series of the *V5-Rluc(Stop)-X-(noAUG)FLuc-HA* dual reporters containing the elements in four 3′ UTRs (Supplementary Figure S3). *CRYBB1(13–25)*, *PEX1(7–17)*, *SH2D1A(5–11)* and *GCH1(29–34)* were identified as minimal regions required for the expression of *(no-AUG)Fluc* in *V5-Rluc(Stop)-X-(noAUG)Fluc-HA* reporters (Supplementary Figure S3 and Figure 2A). Western blot analysis detected the Fluc-HA products derived from reporters *V5-Rluc(Stop)-X-(noAUG)FLuc-HA* containing minimal regions of these 3′ UTR elements (Figure 2B), with Fluc activities being consistent with the levels of Fluc-HA determined by western blotting (Figure 2C). V5-Rluc was decreased when Fluc-HA was translated from the reports containing three 3′ UTRs, *CRYBB1(1–25)*, *PEX1(1–17)*, *SH2D1A(1–11)*, but not from the minimal regions required for the expression of downstream Fluc-HA, *CRYBB1(13–25)*, *PEX1(7–17)* and *SH2D1A(5–11)* (Figure 2D). These findings suggest that the reduced expression of upstream Rluc did not correlate with the increased expression of downstream Fluc. The V5-Rluc derived from reporters *V5-Rluc(Stop)-GCH1-(noAUG)FLuc-HA* was not decreased even when Fluc-HA was translated from *GCH1*–3′ UTRs.

To determine whether translation of dORFs in the 3′ UTRs of these mRNAs is conserved in mammals, the various reporters *V5-Rluc(Stop)-X-(noAUG)FLuc-HA* were
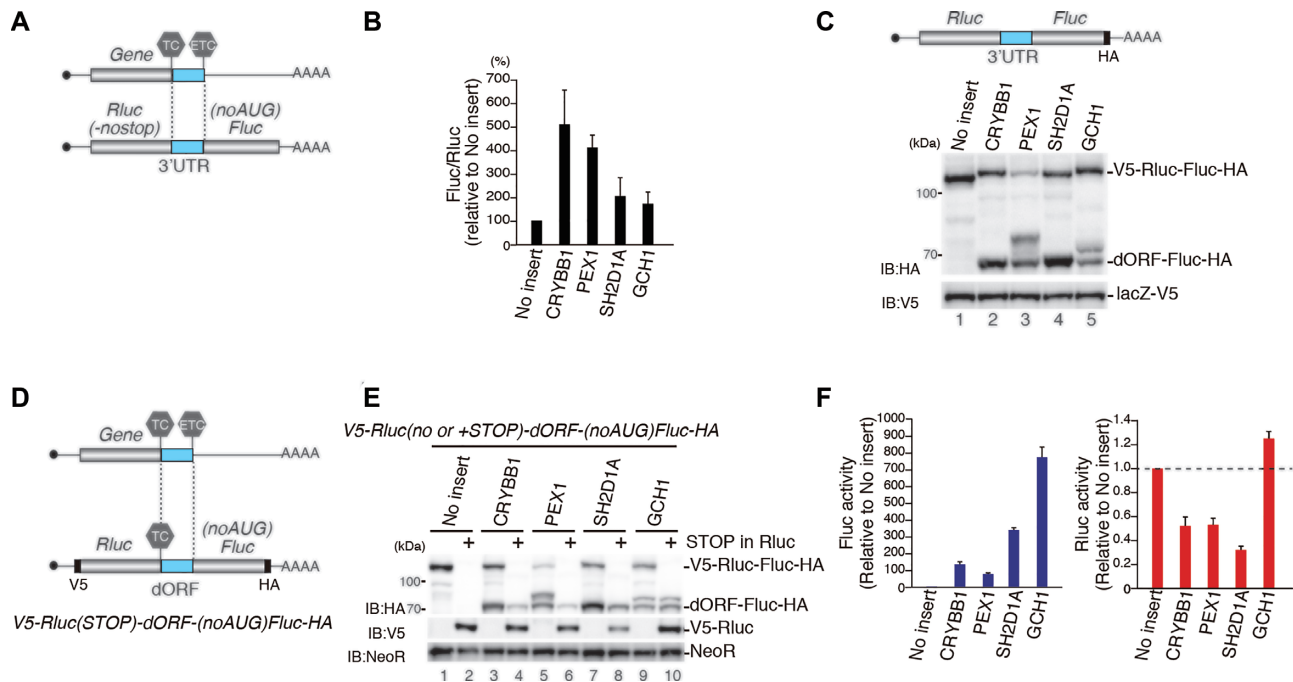
Figure 1. Dual reporter system identification of elements in 3′ UTRs that initiate translation of downstream ORFs. (**A**) Top: Schematic drawing of an mRNA containing a 3′ UTR of genes, in which readthrough mutations (stop codons mutated to sense codons) are responsible for diseases. TC: termination codon; ETC: extended termination codon, defined as the next termination codon after readthrough of the original TC. Bottom: Schematic drawing of the *V5-Rluc(noSTOP)-X-(noAUG)Fluc-HA* dual reporter mRNA containing a 3′ UTR. The gray boxes indicate Rluc and Fluc ORFs, and the blue box indicates an untranslated region (UTR). Rluc contains an AUG initiation codon but not a termination codon. Fluc does not contain an AUG initiation codon at the start of its ORF. (**B**) Translation of downstream Fluc was significantly enhanced by the 3′ UTRs of four genes. Cell lysates were prepared from HEK293T cells harboring the reporters, and the luciferase activities derived from the *V5-Rluc(noSTOP)-X-(noAUG)Fluc-HA* dual luciferase reporters, as well as the ratio of luciferase activities of the reporters with four 3′ UTRs, were determined. Results reported are the mean ± S.D. of three independent experiments. (**C**) Production of full-length Rluc-X-FLuc fusion proteins and Fluc proteins from *V5-Rluc(noSTOP)-X-(noAUG)Fluc-HA* reporters following insertion of four 3′ UTRs. Top: Schematic drawing of the *V5-Rluc(noSTOP)-X-(noAUG)Fluc-HA* reporters. HA-tag was inserted upstream of a termination codon to allow detection of products by western blotting. Bottom: Western blot analysis showing the Fluc products derived from *V5-Rluc(noSTOP)-X-(noAUG)Fluc-HA* reporters with the insertion of four 3′ UTRs. Lysates were prepared from HEK293T cells harboring the reporters, and the products were detected with anti-HA antibody (Top panel). The expression levels of co-transfected *lacZ-V5* were determined with anti-V5 antibody. (**D**) Schematic drawing of the *V5-Rluc(noSTOP)-X-(noAUG)Fluc-HA* dual reporter mRNA that contains a 3′ UTR. The gray boxes indicate Rluc and Fluc ORFs, and the blue box indicates a UTR. *V5-Rluc(STOP)* contained both an initiation and a termination codon, whereas *(noAUG)Fluc-HA* did not contain an AUG initiation codon at the start of the ORF. (**E**) Western blot analysis of full-length Rluc-X-FLuc fusion proteins and Fluc proteins from *V5-Rluc(STOP)-X-(noAUG)Fluc-HA* reporters into which four 3′ UTRs had been inserted. Lysates were prepared from HEK293T cells harboring the reporters, and the products were detected with anti-HA antibody (Top panel). The expression levels of NeoR proteins derived from the transfected plasmids were determined with anti-neomycin phosphotransferase2 antibody (bottom panel). (**F**) Translation of downstream Fluc was significantly enhanced by the 3′ UTR of four genes. Fluc (left panel) and Rluc (right panel) luciferase activities derived from the *V5-Rluc(STOP)-X-(noAUG)Fluc-HA* reporters, as well as their ratios, were determined. Results reported are the mean ± S.D. of three independent experiments.

transfected into mouse Neuro 2A cells. Western blot analysis detected Fluc-HA products derived from reporters containing *CRYBB1(13–25)*, *PEX1(7–17)*, *SH2D1A(5–11)* and *GCH1(29–34)* (Supplementary Figure S4), indicating that dORFs in the 3′ UTR could be translated in various cell lines, and that the minimal regions required for the expression of dORFs were conserved. The putative dORFs in these four genes were also identified in the mouse genome, leading to the construction of the reporters *V5-Rluc-X-(noAUG)FLuc-HA* and *V5-Rluc(Stop)-X-(noAUG)FLuc-HA* containing the elements in the four 3′ UTRs of mice (Supplementary Figure S5A). Western blot analysis of HEK293T cells transfected with these reporters detected the Fluc-HA products from the reporters containing the elements in the 3′ UTRs of the mouse *SH2D1A* and *GCH1* genes, mSH2D1A and mGCH1, respectively (Supplementary Figure S5B, lanes 7–10). These suggest that translation

of dORFs in the 3′ UTRs of these mRNAs is conserved in mammals.

The mechanism underlying the translation of dORFs was assessed by determining the codons from which translation was initiated. AUG codons were detected in the minimal regions of 3′ UTR elements of *PEX1* and *GCH1* required for the expression of downstream *(no-AUG)Fluc-HA*. Mutation of codon 14 (AUG) of *PEX1* to GGG completely suppressed the expression of Fluc (Figure 2E, lane 2), indicating that translation of downstream *(no-AUG)Fluc-HA* requires an AUG codon. Two distinct dORF-Fluc products were expressed from the reporter containing the 3′ UTR of *GCH1*, with the larger and smaller products named L-dORF-Fluc-HA and M-dORF-Fluc-HA, respectively (Figure 2E). Mutation of codon 34 (AUG) of *GCH1* to GGG completely suppressed the expression of M-dORF-Fluc-HA (Figure 2E, lane 4), indicating that the transla-
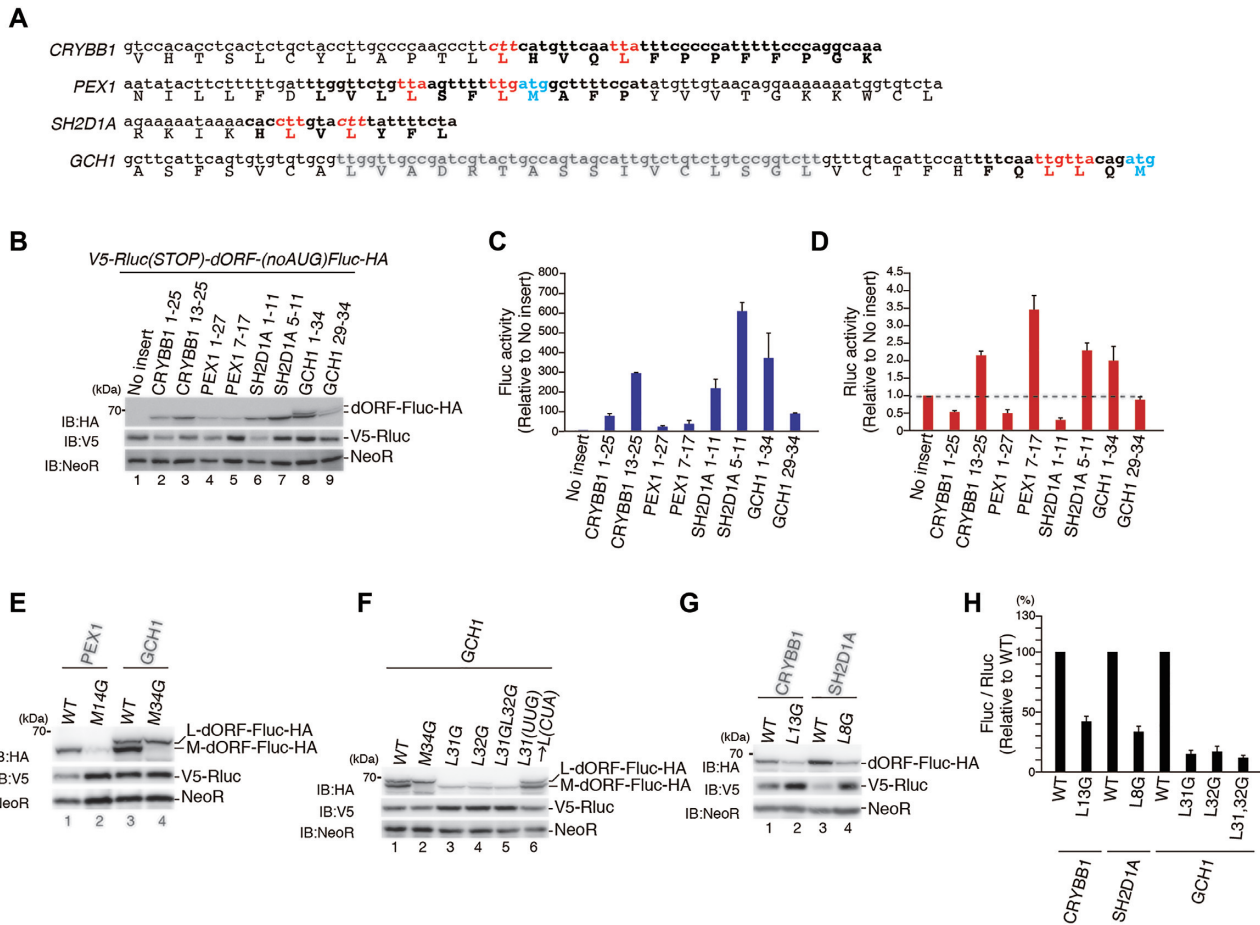
Figure 2. Initiation codons for dORF translation in 3′ UTRs. (**A**) Sequences of minimal regions required for the expression of *(no-AUG)Fluc* from *V5-Rluc(Stop)-X-(noAUG)Fluc-HA* reporters. The bold letters indicate the minimal regions of the 3′ UTRs of *CRYBB1(13–25)*, *PEX1(7–17)*, *SH2D1A(5–11)* and *GCH1(29–34)* required to induce the expression of *(no-AUG)Fluc-HA*. The red letters indicate the initiation codons required for the expression of *(no-AUG)Fluc-HA*. Leu initiation codon mutations affected 3′ IRES-mediated translation activity. (**B**) Western blot analysis of the Fluc products derived from the *V5-Rluc(Stop)-X-(noAUG)Fluc-HA* reporters containing the minimal regions of these four 3′ UTRs. Lysates were prepared from HEK293T cells harboring these reporters; the Fluc-HA products were detected with anti-HA antibody (Top panel), and the V5-Rluc products were detected with anti-V5 antibody (middle panel). The expression levels of NeoR proteins derived from the transfected plasmids were determined with anti-neomycin phosphotransferase2 antibody (bottom panel). (**C** and **D**) Translation of downstream Fluc was significantly enhanced by the minimal regions of 3′ UTRs. Fluc (C) and Rluc (D) luciferase activities derived from the *V5-Rluc(STOP)-X-(noAUG)Fluc-HA* reporters were determined. Results reported are the mean ± S.D. of three independent experiments. (**E–G**) Western blot analysis of Fluc products derived from the *V5-Rluc(Stop)-X-(noAUG)Fluc-HA* reporters. Lysates were prepared from HEK293T cells harboring these reporters; the Fluc-HA products were detected with anti-HA antibody (top panel), and the V5-Rluc products were detected with anti-V5 antibody (middle panel). The expression levels of NeoR proteins derived from the transfected plasmids were determined with anti-neomycin phosphotransferase2 antibody (bottom panel). (E) AUG codons in the minimal regions of *PEX1* and *GCH1* 3′ UTR elements required for the expression of downstream *(no-AUG)Fluc-HA*. (**F**) Initiation of translation of downstream *(no-AUG)Fluc-HA* of the V5-*Rluc(Stop)-GCH1-(noAUG)FLuc-HA* reporter from the UUG (Leu) codon. (**G**) Initiation of translation of the downstream *(no-AUG)Fluc-HA* reporter from the CUU (Leu) codons within the minimal regions of *CRYBB1* and *SH2D1A*. (**H**) Leu codon-dependent initiation of dORF translation repressed the translation of main ORF. Their ratios derived from the indicated *V5-Rluc(STOP)-X-(noAUG)FLuc-HA* reporters with the four 3′ UTRs, were determined. Results reported are the mean ± S.D. of three biological replicates.

tion of *(no-AUG)Fluc-HA* is initiated from this codon. L-dORF-Fluc-HA was still produced from V5-*Rluc(Stop)-GCH1-(noAUG)FLuc-HA*, with no other AUG codon being present in the minimal region of the 3′ UTR of *GCH1*. These findings suggest that translation may be initiated from a non-AUG codon, such as two Leu codons. Mutation of codons 31 (UUG) and 32 (UUA) of *GCH1* to GGG almost completely suppressed the expression of M-dORF-Fluc-HA (Figure 2F, lanes 3–4 and H), whereas mutation of codon 31 (UUG) to CUA, both encoding Leu, did not affect the expression of the upper dORF-Fluc-HA product (Figure 2F, lane 6), suggesting that both Leu-encoding codons, CUA and UUA, initiate translation of

dORF. These findings strongly suggest that translation of the downstream *(no-AUG)Fluc-HA* reporter starts from the UUG Leu-encoding codon. The Leu initiation codons UUG/UUA for the expression of L-dORF-Fluc-HA are close to the AUG initiation codon. It was therefore surprising that the translation products of L-dORF-Fluc-HA and M-dORF-Fluc-HA could be separated on PAGE (Figure 2E, lane 3, Figure 1C, lane 5 and Figure 1E, lane 10). The reason for the difference in migration between these two products is unclear, but it may be due to differences in their amino acid compositions. The minimal regions of *CRYBB1* and *SH2D1A*, and *CRYBB1(13–25)* and *SH2D1A(5–11)*, respectively, do not contain AUG codons (Figure 2A), sug-

gesting that translation of mRNAs encoded in these minimal regions may be initiated from Leu codons. The replacement of codon 13 (CUU, encoding Leu) of *CRYBB1* and codon 8 (CUU) of *SH2D1A* by GGG markedly reduced the expression of *(no-AUG)Fluc-HA* (Figure 2G, lanes 2 and 4), strongly suggesting that the translation of the downstream *(no-AUG)Fluc-HA* reporter is initiated from the CUU codons within the minimal regions of *CRYBB1* and *SH2D1A*. Thus, translation of the dORFs in these 3′ UTRs can be initiated from AUG-encoding codons, including codon 14 of *PEX1* and codon 34 of *GCH1*, or from Leu-encoding codons, such as codon 13 of *CRYBB1*, codon 8 of *SH2D1A* and codons 31 and 32 of *GCH1*. The levels of V5-Rluc derived from *V5-Rluc(Stop)-CRYBB1-(noAUG)Fluc-HA* when *CRYBB1* contained Leu but not Gly at codon 13 (Figure 2G, lanes 1–2, middle panel), and the levels of V5-Rluc derived from *V5-Rluc(Stop)-SH2D1A-(noAUG)Fluc-HA*, were reduced when *SH2D1A* contained Leu but not Gly at codon 8 (Figure 2G, lanes 3–4, middle panel). Luciferase activities showed similar patterns (Figure 2H), suggesting that translation of the dORF repressed translation of main ORF in these constructs, and that the elements in 3′ UTRs initiate translation of dORFs.

IRES in 3′ UTR drives translation of dORF

The results shown above suggest that these 3′ UTR elements have the ability to reinitiate translation of dORFs after translation is terminated at a stop codon, or to initiate IRES-mediated translation. To further investigate the mechanism of dORF translation, a sequence that forms a stem-loop structure was inserted into a 5′ UTR, thereby inhibiting the scanning of the 43S preinitiation complex in cap-dependent translation (Figure 3A). The insertion of a stem-loop structure eliminated translation of full-length V5-Rluc(Stop)-X-(noAUG)Fluc-HA (Figure 3B, lanes 3, 7, 11, 15 and 19) and Rluc derived from V5-Rluc(Stop)-X-(noAUG)Fluc-HA products (Figure 3B, lanes 4, 8, 12, 16 and 20), indicating that a stem-loop structure strongly represses cap-dependent translation of Rluc. The insertion of a stem-loop structure into the 5′ UTR of Fluc, however, did not affect the level of dORF-(noAUG)Fluc proteins encoded by *V5-Rluc(Stop)-GCH1 dORF-(noAUG)Fluc-HA* (Figure 3B, lanes 19–20), strongly suggesting that the 3′ UTR of *GCH1* possesses IRES activity that initiates the translation of dORFs. By contrast, the sequence forming a stem-loop structure in the 5′ UTR inhibited the production of *(noAUG)Fluc-HA* proteins encoded by the other three *V5-Rluc(Stop)-X-(noAUG)Fluc-HA* reporters (Figure 3B, lanes 7–8, 11–12 and 15–16). These findings suggest that *(noAUG)FLuc-HA* is translated by re-initiation after termination at a stop codon of *Rluc*.

The efficiency of re-initiation was shown to be inversely proportional to the distance between the termination and re-initiation codons (25). To further investigate the mechanism by which the elements of 3′ UTR facilitate translation of downstream Fluc, the long fragment was inserted just downstream of the translation termination codon of *Rluc* (Figure 3C). The insertion of NanoLuc ORF with-

out AUG (*noAUG-Nluc*) reduced but did not eliminate the generation of the dORF product initiated from the 3′ UTR of *GCH1* (Figure 3D, lanes 5 and 10), and the insertion of a noAUG insert derived from the Nluc sequence eliminated the generation of the dORF product initiated from the other three 3′ UTR elements (Figure 3D, lanes 2–4 and 7–9). The amount of NeoR was consistently lower than that in the absence of the insert, probably due to the less efficient transfection of the longer plasmid. The luciferase activities derived from the reporters demonstrated that the level of dORF-(noAUG)Fluc protein resulting from translation of the *V5-Rluc(Stop)-noAUG-Nluc-GCH1-dORF-(noAUG)Fluc-HA* reporter was reduced by the insertion of the *noAUG-Nluc* fragment. By contrast, dORF-(noAUG)Fluc proteins derived from other reporters were almost eliminated by the insertion of the *noAUG-Nluc* fragment (Figure 3E). Because the efficiency of re-initiation is inversely proportional to the distance between the termination and re-initiation codons (26), the *V5-Rluc(Stop)-noAUG-Nluc-X-dORF-(noAUG)Fluc-HA* reporters containing the 3′ UTR elements of *CRYBB1*, *PEX1* and *SH2D1A* were translated by re-initiation to yield dORF-Fluc-HA products. The insertion of a stem-loop structure into the 5′UTR and the long fragment just after the termination codon of the upstream ORF did not strongly repress the production of *GCH1*-dORF-Fluc-HA, suggesting that the 3′-UTR of *GCH1* possesses IRES activity.

We also investigated mRNAs produced from the *Rluc(noSTOP)-X-(noAUG)FLuc* dual reporters with Northern blotting using *FLUC* probe. The full-length and truncated mRNAs derived from the *Rluc(noSTOP)-dORF-(noAUG)FLuc* reporters were detected (Supplementary Figure S6A, lanes 4, 7, 10 and 13). The insertion of a stem-loop structure significantly reduced the levels of both full-length *V5-Rluc(Stop)-X-(noAUG)Fluc-HA* mRNAs and the truncated mRNA derived from *V5-Rluc(Stop)-X-(noAUG)Fluc-HA* (Supplementary Figure S6A, lanes 6, 9, 12 and 15). The insertion of termination codon into the Rluc also significantly reduced the levels of full-length and truncated mRNAs (Supplementary Figure S6A, lanes 5, 8, 11 and 14), probably due to the nonsense-mediated mRNA decay. Importantly, the levels of the truncated mRNAs correlated with that of the full-length mRNAs in these constructs, suggesting that the truncated mRNAs are derived from the full-length mRNAs. The primer extension experiments determined the 5′ ends of the truncated mRNAs derived from V5-Rluc(Stop)-X-(noAUG)Fluc-HA reporters containing the 3′ UTR elements of *CRYBB1*, *PEX1* and *SH2D1A* (Supplementary Figures S6B and C). The 5′ ends were mapped within the Rluc ORF, upstream of the dORF insertion, suggesting that the truncated mRNAs were not produced by promoter activity of the dORF insertion. The 5′ end of the truncated mRNAs derived from *V5-Rluc(Stop)-GCH1-(noAUG)Fluc-HA* reporters were mapped within the insertion but upstream of the *cis*-element required for the production of GCH1-dORF-Fluc-HA (Supplementary Figures S6B and C). We propose that translation of 3′UTR inhibits 5′ to 3′ decay and results in the production of the truncated mRNAs.
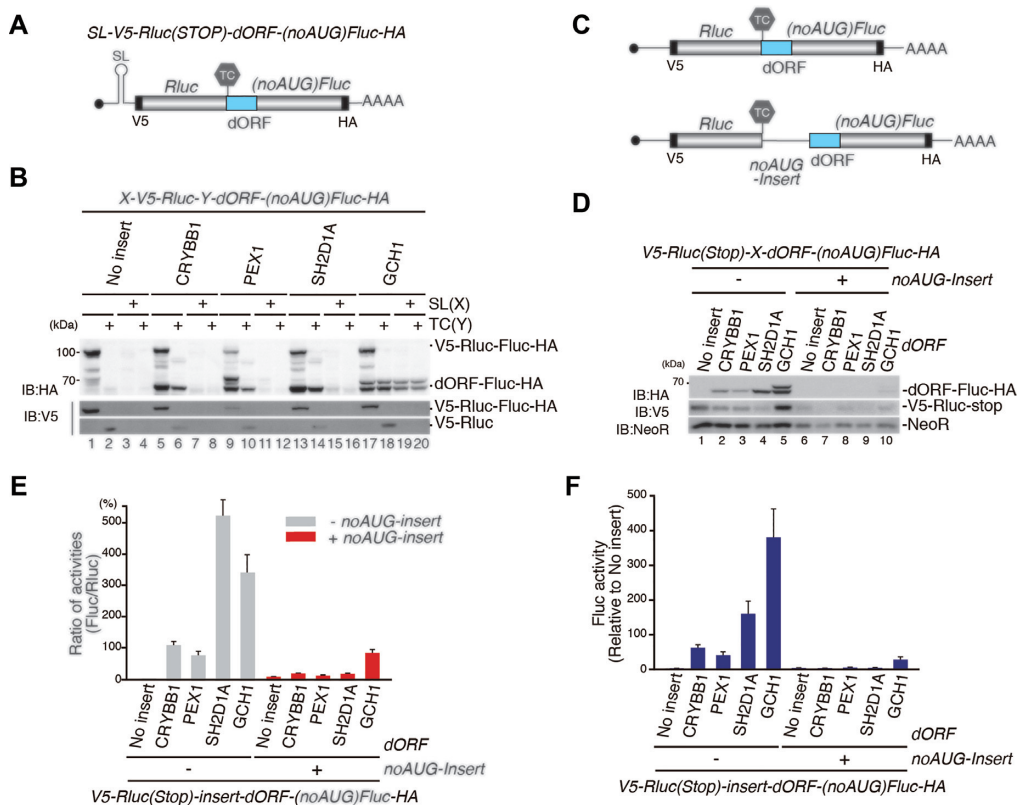
Figure 3. IRES in 3′ UTR drives translation of dORF. (**A**) Schematic drawing of the *SL-V5-Rluc(STOP)-(noAUG)Fluc-HA* dual reporter mRNA. SL, sequence forming a stem-loop structure. The gray boxes indicate Rluc and Fluc ORFs, and the blue box indicates a UTR. *V5-Rluc(STOP)* contains both an initiation and termination codon, whereas *(noAUG)Fluc-HA* does not contain an AUG initiation codon at the start of the ORF. (**B**) Western blot analysis of dORF-Fluc-HA products derived from various *X-V5-Rluc(STOP)-Y-(noAUG)Fluc-HA* reporter mRNAs, with X = SL indicating an element that forms a stem-loop structure and Y = TC indicating V5-Rluc with a termination codon. Lysates were prepared from HEK293T cells harboring these reporters, and dORF-Fluc-HA and NeoR proteins were determined with anti-HA (top panel) and anti-V5 (bottom panel) antibodies. (**C**) Schematic drawing of *SL-V5-Rluc(STOP)-(noAUG)Fluc-HA* reporter mRNAs without (top) and with (bottom) an inserted (noAUG)Nluc lacking an AUG codon. (**D**) Western blot analysis of dORF-Fluc-HA products derived from various *V5-Rluc(Stop)-X-(noAUG)FLuc-HA* reporter mRNAs. Lysates were prepared from HEK293T cells harboring these reporters, and dORF-Fluc-HA and NeoR proteins were determined with anti-HA (top panel) and anti-neomycin phosphotransferase2 (bottom panel) antibodies. (**E** and **F**) Expression of Fluc-HA (E) and the ratio of Fluc to Rluc (F) by *V5-Rluc(Stop)-GCH1-(noAUG)FLuc-HA* reporters with a stem-loop structure in the 5′ UTR or an inserted long fragment just after the termination codon of Rluc. –noAUG-Nluc (gray box) and +noAUG-Nluc (red box) luciferase activities derived from the indicated *V5-Rluc(STOP)-X-(noAUG)Fluc-HA* dual luciferase reporters with the four 3′ UTRs, as well as their ratios, were determined. Results reported are the mean ± S.D. of three independent experiments.

eIF4G drives AUG-dependent 3′ IRES activity of *GCH1* in the reconstituted translation system

The mechanism of dORF translation from the 3′ UTR of *GCH1* was investigated using a reconstituted *in vitro* translation system (27). The template mRNAs were m7G-capped and A-capped *V5-Ruc(STOP)-X-(noAUG)Nluc-HA* mRNAs containing Rluc ORF followed by the 3′ UTR of *GCH1* and Nluc ORF lacking an AUG codon (Figure 4A). The controls included m7G-capped and A-capped *V5-Rluc-(noAUG)Nluc-HA* mRNAs, which produced Rluc-Nluc fusion proteins (Figure 4B). With m7G-capped mRNAs, the ratio of Nluc-to-Rluc activity was 40% that of control *V5-Rluc-(noAUG)Nluc-HA* mRNA (Figure 4B, gray bars). HCV-IRES, the prototype of structurally similar type 3 viral IRESs, binds directly to the 40S rRNA subunit and eIF3 (28) via several IRES structural domains (29–32), along with the eIF2-containing ternary complex, resulting in the formation of a 43S preinitiation complex (PIC) and

an elongation-competent 80S ribosome (18). As expected, HCV-IRES strongly facilitated the translation of Nluc from both m7G-capped and A-capped reporter mRNAs (Figure 4B). With A-capped mRNAs, the ratio of Nluc-to-Rluc activity was 50% that of control *V5-Rluc-(noAUG)Nluc-HA* mRNA, indicating that the 3′ UTR of *GCH1* contains cap-independent IRES activity (Figure 4B, *GCH1* bars). The IRES activity of the 3′ UTR of *GCH1* with A-capped mRNA was almost the same as that of CrPV-IRES and 10% that of HCV-IRES (Figure 4B). The 3′ UTR of *GCH1* produced Nluc protein from both m7G-capped and A-capped *V5-Rluc(STOP)-X-(noAUG)Nluc-HA* mRNAs (Figure 4C, red bars in *GCH1*), although the amount of Rluc protein produced by A-capped mRNA was significantly reduced due to the m7G-cap-dependent translation of Rluc (Figure 4C, gray bars in *GCH1*).

We next investigated the function of translation initiation factors for *GCH1*-IRES. eIF4F is required for translation of both luciferase reporters of A-capped *V5-Rluc(STOP)-*
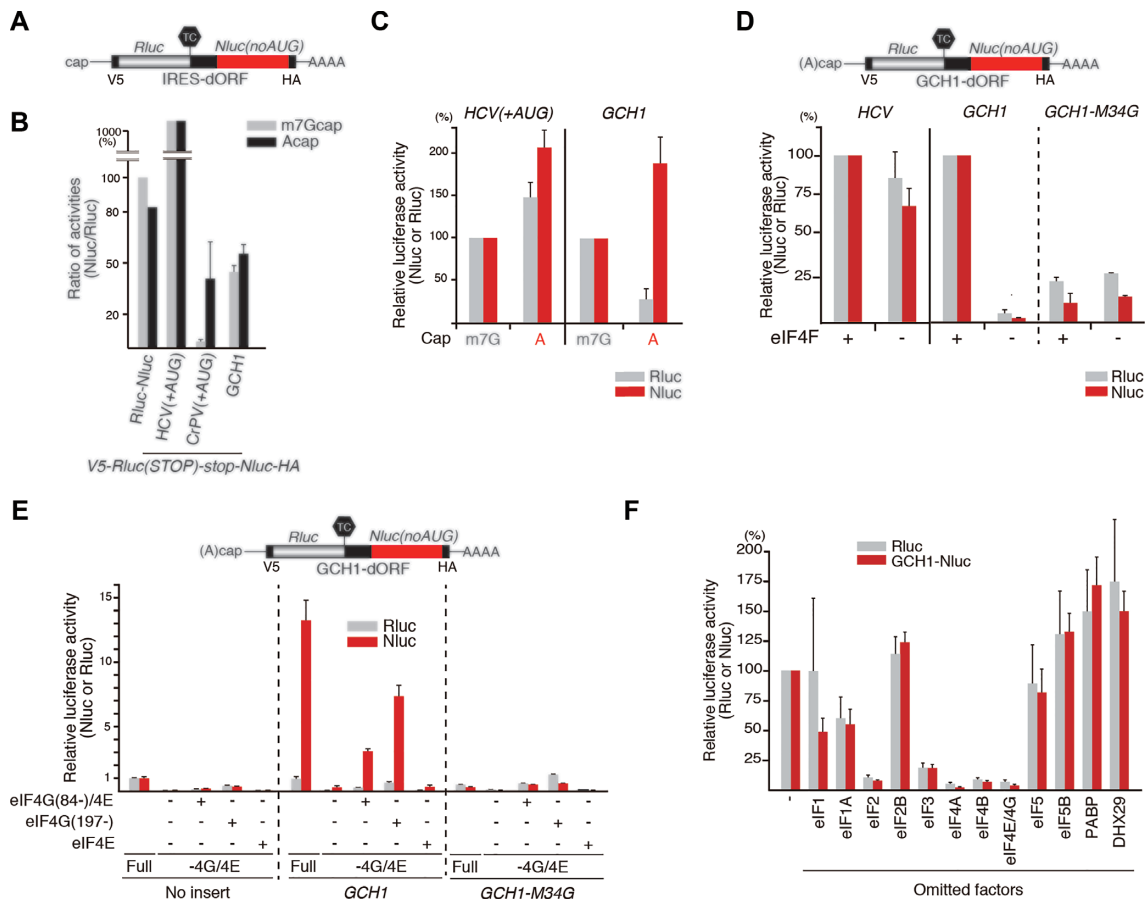
Figure 4. eIF4G drives AUG-dependent 3′ IRES activities in the reconstituted translation system. (**A**) Schematic drawing of the *V5-Rluc(STOP)-IRES-(noAUG)Nluc-HA* dual reporter mRNA for *in vitro* translation assays. The gray box indicates Rluc, the red box indicates Nluc, and the black box indicates IRESs. *V5-Rluc(STOP)* contains both an initiation and termination codon, whereas *(noAUG)Nluc-HA* lacks an AUG initiation codon at the start of the ORF. (**B**) Expression of Nluc-HA by m7G or A-capped reporter mRNAs. The luciferase activities of Rluc and Nluc derived from the indicated mRNAs, as well as their ratios, were determined. (C–F) *In vitro* translation in the reconstituted translation system. (C) 3′ UTR of *GCH1* contains cap-independent IRES activity. Determination of the Nanoluc activities of Nluc products derived from the indicated m7G-capped and A-capped reporter mRNAs with HCV-IRES or 3′ UTR of *GCH1*. (**D**) Dependence of cap-independent IRES activities of the 3′ UTR of *GCH1* on an AUG initiation codon and eIF4F. The Nanoluc activities of Nluc products derived from the indicated A-capped reporter mRNAs with HCV-IRES or 3′ UTR of *GCH1* were determined. (**E**) Dependence of cap-independent IRES activity of the 3′ UTR of *GCH1* on eIF4G but not on eIF4E. The Nanoluc activities of Nluc derived from the *V5-Rluc(STOP)-GCH1-(noAUG)Nluc-HA* were determined in the reconstituted translation system in the presence or absence of eIF4G. (**F**) 3′-IRES activity of *GCH1* depends on eIF2, eIF3, eIF4A, eIF4B and eIF4G. Nanoluc activities derived from the indicated A-capped *V5-Rluc(STOP)-GCH1-(noAUG)Nluc-HA* mRNAs with 3′ IRES-*GCH1* were determined in the reconstituted translation system following omission of each indicated translation factor. Results reported are the mean ± S.D. of Nluc amounts normalized to Rluc amounts from three independent experiments.

GCH1-(noAUG)Nluc-HA mRNA (Figure 4D), although HCV-IRES significantly facilitated the translation of the *(noAUG)Nluc-HA* reporter in the absence of eIF4F. These findings indicate that the IRES in the 3′ UTR of *GCH1* requires eIF4F for initiation of translation. Replacement of the AUG sequence at codon 34 with GGG eliminated the expression of both reporters, indicating that an internal AUG codon in the 3′ UTR of *GCH1* is required for IRES-mediated translation of Nluc and Rluc (Figure 4D). Since the eIF4F-dependent *GCH1*-IRES activity was observed with A-capped mRNA, the eIF4E dependence of IRES activity on *GCH1* was investigated (Figure 4E). Translation of Nluc depended on eIF4F, with reduced translation restored by the addition of eIF4G(84–1599)+eIF4E and eIF4G(197–1599) alone, but not by eIF4E alone, indicating that *GCH1*-IRES activity requires eIF4G but does not

require eIF4E or cap structure (Figure 4E, middle panel). These findings indicated that the 3′ UTR of *GCH1* contains an eIF4G-dependent IRES (3′ IRES) and dORF. Substitution of the AUG at codon 34 with GGG again eliminated the expression of both reporters (Figure 4E, right panel), suggesting that AUG-dependent, but not UUG-dependent, initiation of translation could be recapitulated by the reconstituted *in vitro* translation system.

Individual omission of translation factors revealed that *GCH1*–3′ IRES activity was greatly dependent on eIF2, eIF3, eIF4A, eIF4B and eIF4G, but not on eIF4E, eIF1, eIF1A, eIF2B, eIF5, eIF5B, PABP, or DHX29 (Figure 4F). eIF4G may bind directly to the 3′ IRES of *GCH1* and recruit the 43S preinitiation complex, composed of the 40S subunit and the translation factors eIF2, eIF3, eIF4A and eIF4B.

Detection of the 80S initiation complex by toeprinting with Rabbit Reticulocyte Lysate (RRL)

To examine whether GCH1–3′ IRES was associated with the formation of the 48S or 80S initiation complex, primer extension was performed, and the RNP complexes that formed on A-capped RNAs containing short uORF(MVHL) were analyzed, following HCV-IRES or GCH1–3′ IRES and NanoLuc ORF (Supplementary Figure S7A). In vitro translation of the A-capped RNAs containing short uORF (MVHL) followed the elements. NanoLuc ORF revealed that the indicated elements between short ORF and NanoLuc ORF moderately but significantly facilitated the translation of the reporter RNAs (Supplementary Figure S7B). Under this condition, the activity of GCH1–3′ IRES was comparable to that of HCV. Moreover, GCH1–3′ IRES-mediated translation was diminished by the M34G mutation (Supplementary Figure S7B), suggesting that GCH1–3′ IRES-mediated translation depended on the AUG initiation codon. Primer extension analysis of RNP complexes formed on HCV-IRES and the 3′-GCH1-element with the 5′ fluorescence-labeled primer showed that toeprinting with HCV-IRES occurred following incubation with RRL, as previously demonstrated (Supplementary Figure S7C, lanes 1–2). The position of the toeprinting signal was shifted in the presence of the translation inhibitor cycloheximide (CHX) (Supplementary Figure S7C, lanes 2–3), indicating formation of the 80S initiation complex (5,33–34). The M34G mutation eliminated the toeprinting signal, indicating that the 80S complex was formed with the AUG initiation codon of GCH1–3′ IRES at the P-site (Supplementary Figure S7D, lanes 3 and 6). The toeprinting experiments with the reconstituted translation factors failed to detect the 48S initiation complex (data not shown).

eIF4G drives translation initiation by polyU and poliovirus type 2 (PV2) in the reconstituted translation system

PolyU has been hypothesized to directly recruit eIF4G, and short element of PV2 are thought to base pair with 18S rRNA to initiate translation (20). We investigated whether polyU and PV2 facilitate translation initiation in the reconstituted translation system using A-capped *V5-Rluc(STOP)-PV2-(noAUG)Nluc-HA* mRNA (Figure 5B). Translation of Nluc depended on eIF4F, with reduced translation restored by the addition of eIF4G(197–1599) alone or eIF4G(84–1599) plus eIF4E, but not by eIF4E alone, indicating that PV2 activity requires eIF4G but not eIF4E or the cap structure (Figure 5A, left panel). Investigation of polyU activity using A-capped *V5-Rluc(STOP)-polyU-(noAUG)Nluc-HA* mRNA showed that the translation-stimulation activity of polyU was lower than that of PV2, but that polyU activity also required eIF4G but not eIF4E or the cap structure (Figure 5A, right panel). Individual omission of translation factors showed that IRES activity of polyU and PV2 was highly dependent on eIF2, eIF3, eIF4A, eIF4B and eIF4G, but not on eIF4E, eIF1, eIF1A, eIF2B, eIF5, eIF5B, PABP, or DHX29 (Figure 5B and C). The initiation factor dependency of these two elements was similar to that of *GCH1–3′* IRES. Because polyU binds to eIF4G in yeast (35), we
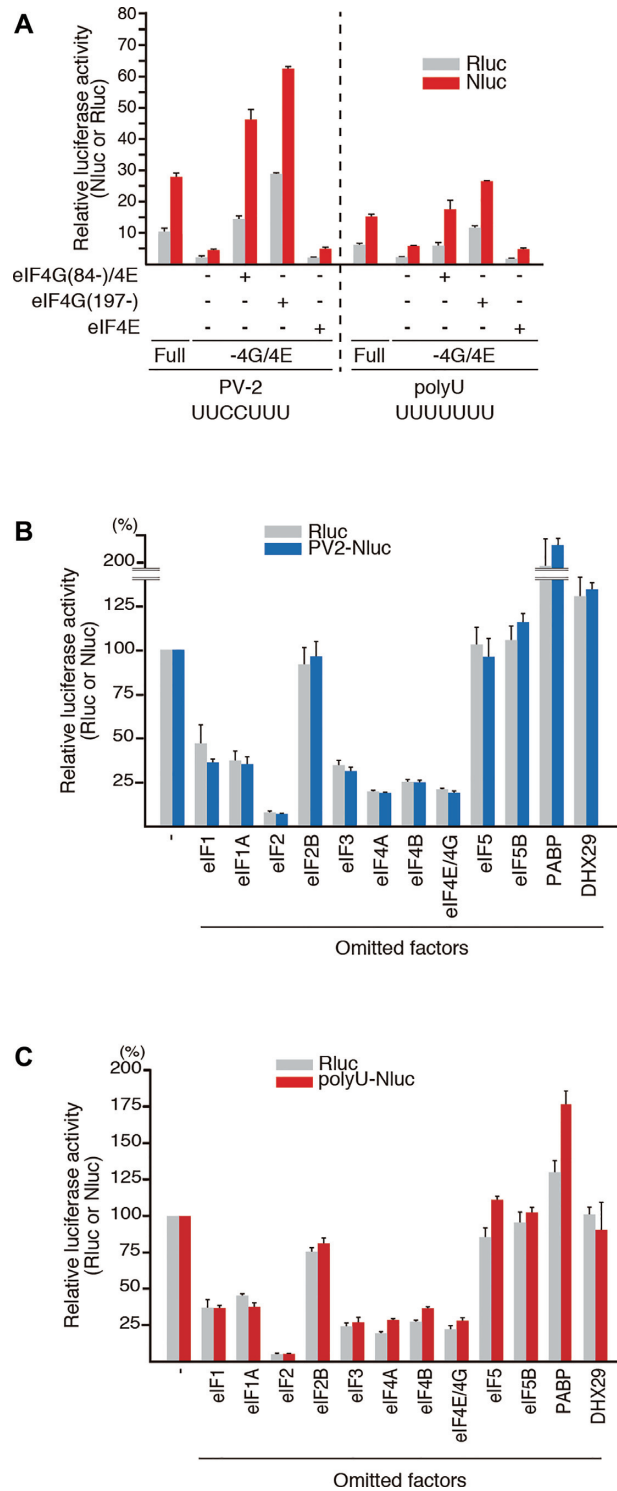

Figure 5. eIF4G drives the IRES activity of PV2 and polyU in the reconstituted translation system. (**A**) Dependence of cap-independent IRES activities of PV2 and polyU on eIF4G but not on eIF4E. The Nanoluc activities derived from the *V5-Rluc(STOP)-PV2/polyU-(noAUG)Nluc-HA* were determined in the reconstituted translation system in the presence or absence of eIF4G. (**B** and **C**) Dependence of the IRES activities of PV-2 and polyU on eIF2, eIF3, eIF4A, eIF4B and eIF4G. Nanoluc activities of the indicated A-capped *V5-Rluc(STOP)-PV2-(noAUG)Nluc-HA* (**B**) and *V5-Rluc(STOP)-polyU-(noAUG)Nluc-HA* (**C**) mRNAs were determined in the reconstituted translation system following omission of each indicated translation factor. Results reported are the mean ± S.D. of three independent experiments.

hypothesized that eIF4G directly binds to *GCH1*–3′ IRES, and polyU and PV2 elements recruit the 43S preinitiation complex, composed of the 40S subunit and translation factors.

3′ IRES-mediated translation is resistant to the mTOR inhibitor Torin 1

The results of reconstituted *in vitro* translation suggest that inhibition of binding of eIF4E to the cap structure could increase the 3′ IRES activity of *GCH1*. The PI3K-Akt-mTOR signaling pathway is a master regulator of RNA translation. Torin 1 is a potent and selective ATP-competitive inhibitor of mTOR (36,37). We therefore assessed the effect of Torin1 on IRES activity using the reporter *V5-Rluc-HCV-IRES-AUG-(noAUG)Fluc-HA* (Figure 6A). Torin 1 effectively blocked the phosphorylation of 4EBP1/2 by mTORC1 and mTORC2 (38,39), suppressing cap-dependent translation in a manner dependent on the non-phosphorylated form of 4EBP1/2. Rluc levels were inversely correlated with Torin1 concentrations (Figure 6B, middle panel), due to the reduced levels of phosphorylated 4E-BP (Figure 6B, lower panel). By contrast, HCV-IRES remained active and translated dORF-Fluc (Figure 6B, upper panel). The level of expression of dORF-Fluc was also reduced, but less efficiently than that of Rluc, increasing the Rluc-to-Fluc ratio as a function of Torin 1 concentration (Figure 6C). Similar results were obtained with IRES of encephalomyocarditis virus (EMCV) (Figure 6D–F). Evaluation of the effects of Torin1 on *GCH1* 3′ IRES-mediated translation showed that the levels of dORF-Fluc were similar, even in the presence of Torin 1, although Rluc levels were reduced (Figure 6H), and the ratio of Rluc-to-Fluc activity was increased as a function of Torin1 concentration (Figure 6I). These findings indicated that *GCH1*–3′ IRES-dependent translation of dORF occurred even when cap-dependent translation of the main ORF was inhibited *in vivo*.

DISCUSSION

A reduction in the levels of releasing factors could induce readthrough of termination codons, enhance specific cis-elements that inhibit termination of translation and/or increase the expression of suppressor tRNAs (25,40–41). Translation of 3′ UTRs in mammalian cells may be aberrant, as the production of C-terminus extended abnormal proteins is generally suppressed. Translation of 3′ UTRs in yeast cells and the synthesis of dORF products also require re-initiation of translation after its termination, a re-initiation resulting from the inhibition of quality control factors (42). A relatively high frequency of genes, including highly expressed ribosomal subunit proteins, undergo translational readthrough and have a higher proportion of intrinsically disordered C-termini. In this study, translational readthrough was observed, but dORF products derived from translation initiation sites in four 3′ UTRs were identified. Translation of dORFs from three of these 3′ UTR elements required re-initiation from non-AUG codons. In yeast, Tma64/eIF2D, Tma20/MCT-1 and Tma22/DENR recycle post-termination 40S subunits (41), and 40S ribosomes appeared to rejoin with 60S subunits and undergo an 80S re-initiation process in 3 UTRs. In mammals, re-initiation and other unconventional post-termination events have been recapitulated by *in vitro* translation using a reconstituted mammalian translation system (25). The presence of eIF2, eIF3, eIF1 eIF1A, and Met-tRNAiMet was sufficient for recycled 40S subunits to remain on mRNA, scanning bidirectionally, and reinitiate at upstream and downstream AUGs if mRNA regions flanking the stop codon were unstructured. We hypothesize that the *cis*-elements required to induce re-initiation in 3′ UTRs were similar in sequence and pyrimidine-rich, suggesting that putative trans-factor(s) may be involved in the re-initiation of translation and the synthesis of dORF products, probably inhibiting the function of those 40S ribosomal subunit recycling factors. The luciferase assays revealed that the levels of Rluc were reduced when Fluc was translated from three 3′ UTRs, *CRYBB1*, *PEX1* and *SH2D1A*. These results strongly suggest that these regions have both initiation codons and activities, enabling translation from these codons. The translation of dORFs repressed the translation of upstream ORFs, suggesting that dORF products regulate the translation of main ORFs.

Translation of dORF from the *GCH1*–3′ UTR element required AUG codons and a termination codon, suggesting that translation initiates from the element but re-initiation does not. Promoter assays showed the absence of cryptic promoters, as the three 3′ UTRs had no activity. *GCH1*–3′ UTR had residual activity, but this activity was significantly lower than that of the CMV promoter. The expression level of the (no-AUG)Fluc derived from the *V5-Rluc(Stop)-GCH1-(noAUG)Fluc-HA* reporter was much higher, comparable to the level of V5-Rluc-Fluc-HA of the control V5-Rluc-(noAUG)Fluc-HA reporter. These findings suggest that cryptic promoter activity does not sufficiently account for the expression of downstream Fluc by the *GCH1*–3′ UTR element. We therefore assessed whether the *GCH1*–3′ UTR element could initiate translation with the reconstituted translation system and performed toeprinting experiments with RRL.

Biochemical approaches have shown that the mechanisms responsible for internal initiation of different classes of IRESs vary greatly, as revealed by their varying requirements for canonical initiation factors and/or specific stimulatory ITAFs. The formation of the 48S initiation complex on type II IRESs such as EMCV-IRES, requires the 43S complex, which is composed of eIF2, eIF3, the 40S ribosomal subunit, the RNA helicase eIF4A, and the central domain of eIF4G (3–6). Synthesis, however, is only moderately stimulated by eIF4B, eIF1 and eIF1A, and does not require the cap-binding protein eIF4E or the N-terminal domain of eIF4G, to which it binds. The potential cellular IRES elements can be classified into three cis-regulatory elements, including polyU and poliovirus type 2 (PV2) short IRES elements (20). However, these IRESs in cellular mRNAs have not been confirmed functionally or biochemically, and assessments of potential cellular IRES have yielded conflicting results (25,43–45). This study identified the elements in 3′ UTRs required to initiate translation of dORFs. The element in the 3′ UTR of *GCH1* was found to drive translation of the dORF *in vivo* and in the reconstituted translation system, indicating that this element possesses IRES activity, al-
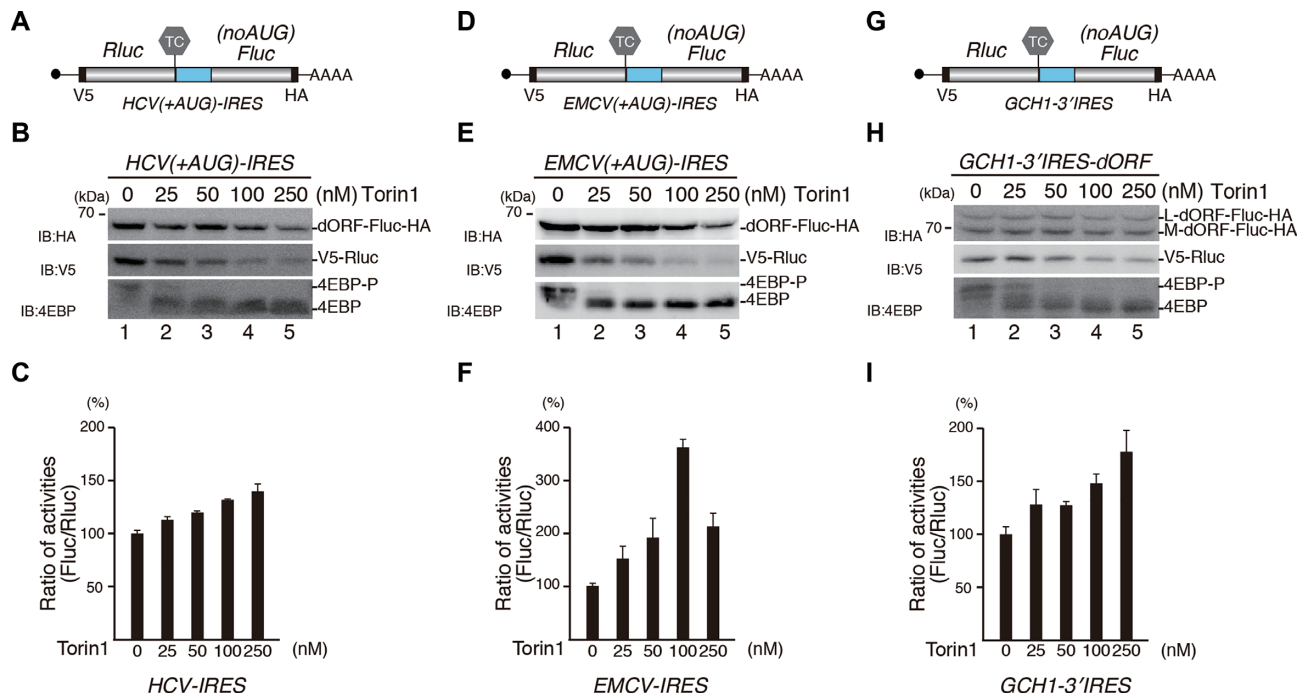
Figure 6. 3' IRES-mediated translation is resistant to mTOR inhibition. (**A**, **D** and **G**) Schematic drawings of the dual reporter mRNAs containing IRESs, *V5-Rluc(STOP)-HCV(AUG)-IRES-(noAUG)Fluc-HA* (A) and *V5-Rluc(STOP)-EMCV(AUG)-IRES-(noAUG)Fluc-HA* (D), and *V5-Rluc(STOP)-3'IRES-GCH1-(noAUG)Fluc-HA* (G). The gray boxes indicate Rluc and Fluc ORFs, and the blue box indicates a UTR. *V5-Rluc(STOP)* contains both an initiation and a termination codon, whereas *(noAUG)Fluc-HA* lacks an AUG initiation codon at the start of the ORF. (**B**, **E** and **H**) Fluc-HA proteins from *V5-Rluc(STOP)-HCV(AUG)-IRES-(noAUG)FLuc-HA* (B) and *V5-Rluc(STOP)-EMCV(AUG)-IRES-(noAUG)FLuc-HA* (E), and *V5-Rluc(STOP)-3'IRES-GCH1-(noAUG)Fluc-HA* (H) reporters with the insertion of GCH1 3' UTRs. Western blot analysis of the Fluc products derived from V5-*Rluc(STOP)-3'IRES-GCH1-(noAUG)Fluc-HA* reporters. Lysates were prepared from HEK293T cells harboring the reporters, and their products were detected with anti-HA antibody (top panel). The expression levels of V5-Rluc were determined with anti-V5 antibody (middle panel), and the expression levels of phosphorylated and non-phosphorylated 4E-BP were determined with anti-4E-BP antibody (bottom panel). (**C**, **F** and **I**) The 3' IRES of GCH1-mediated translation is resistant to mTOR inhibition. Ratios of Fluc-to-Rluc luciferase activities derived from *V5-Rluc(STOP)-HCV(AUG)-IRES-(noAUG)Fluc-HA* (C) and *V5-Rluc(STOP)-EMCV(AUG)-IRES-(noAUG)Fluc-HA* (F), and *V5-Rluc(STOP)-3'IRES-GCH1-(noAUG)Fluc-HA* (I) dual luciferase reporters. Results reported are the mean ± S.D. of three independent experiments.

lowing it to initiate translation of dORF. The *in vitro* reconstituted translation system revealed that the IRES required eIF4G, eIF2, eIF3, eIF4A and eIF4B, but not eIF4E, eIF1, eIF1A, eIF2B, eIF5, eIF5B, PABP, or DHX29 (Figure 4F). The minimal *cis*-element required for IRES activity was 12 nt in length, which may be too short to form the secondary structure required to recruit these factors. Our results suggest that eIF4G binds directly to these elements and recruits the 43S preinitiation complex, which is composed of the 40S subunit and translation factors. The consensus nucleotide sequence for eIF4G recognition remains unclear in mammals, but eIF4G preferentially binds to polyU sequences in yeast (35). One possibility is that the element recruits eIF4G in a manner independent of cap structure and eIF4E. By rearranging the ribosomal 40S subunit head, eIF4G and eIF4A–eIF4B tune the conformational energy landscape of the ribosome to induce opening of the mRNA entry channel. The 3' IRES of *GCH1* may therefore recruit eIF4G, which, together with the RNA helicase activity of eIF4A and eIF4B, unwinds the RNA region needed to initiate translation. The toeprinting experiments with the reconstituted translation factors demonstrated that *GCH1–3'* IRES facilitates the formation of the 80S complex on the AUG initiation codon of *GCH1–3'* IRES at the P-site. The inability to detect the 48S initiation complex suggested that

the 48S ribosome formed at the initiation codon may be below the limit of detection, or that its retention is less stable than that of HCV-IRES. Many of the well-characterized IRESs require canonical initiation factors and specific stimulatory ITAFs. These elements may also require potential ITAFs, suggesting the need for further experiments, including in silico analysis and pull-down assays.

Experiments with the reconstituted translation system suggest that eIF4G generally drives the activity of the polyU and poliovirus type 2 (PV2) short IRES elements, as well as the *GCH1*–3' IRES. Our results also suggest that eIF4G binds directly to the PV2 and polyU elements, and recruits the 43S preinitiation complex, which is composed of the 40S subunit and translation factors. The binding of pyrimidine-rich mRNA sequences to 18S RNA may be similar to the prokaryotic Shine-Dalgarno (SD) sequence (20). Although the ability of PV2-IRES to form base pairs with 18S rRNA has not been determined, our results suggest that eIF4G generally recognizes endogenous IRESs in mRNAs, initiating the translation of uORFs, main ORFs and dORFs. Type II IRES, which require the C-terminal region of eIF4G, contain an A-rich bulge within domain IV, which is absolutely essential for eIF4G binding (46–48). Further experiments should confirm the direct binding of mammalian eIF4G to polyU.
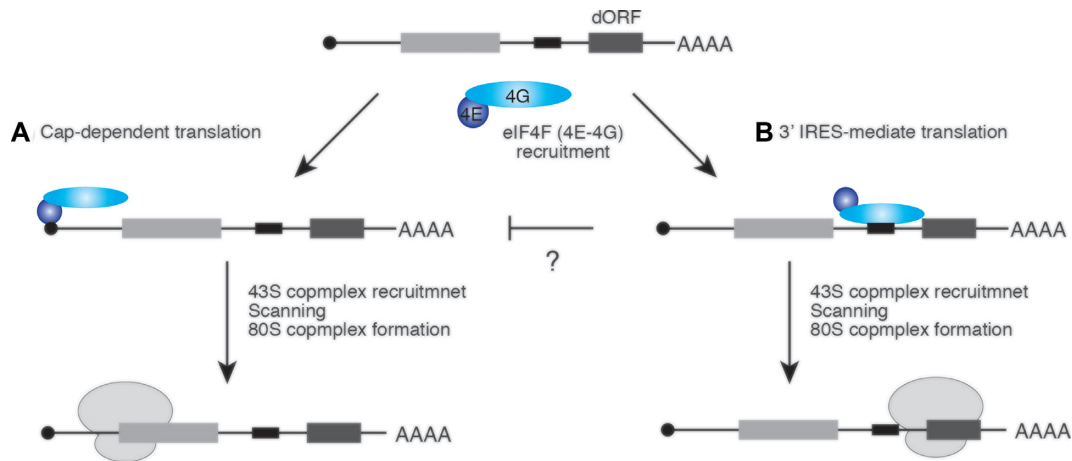
Figure 7. Model for eIF4G-driven initiation of translation from *GCH1*–3′ UTR. The eIF4F complex can bind to mRNA via the cap structure (**A**) or the *GCH1*–3′ UTR element (**B**). The binding of eIF4F to two sites may occur simultaneously or may be competitive. Binding of the eIF4F complex to the cap structure initiates the conventional translation pathway, with translation of upstream ORF from the first AUG codon. Binding of the eIF4F complex to the *GCH1*–3′ UTR element may occur via the binding of eIF4G to an element in eIF4E in a cap-structure-independent manner. Conventional translation factors and 43S ribosome complex are recruited, and 80S complex formation on the 3′UTR initiates translation of dORF.

Cap-independent translation enhancers (CITEs) are also used for the translation of naturally uncapped mRNAs. CITEs are most prevalent in the 3′ UTRs of plant viral mRNAs, where they assume various three-dimensional pseudoknotted structures, facilitating the recruitment of components of the eIF4F complex or ribosomal subunits (49). A comparison of the three mechanisms of translation initiation, cap-dependent translation, IRES, and CITE, suggested a workflow for the validation of IRES activity based on four criteria (47): i) resistance to eIF4G cleavage, ii) resistance to mTORC1 inhibition, iii) resistance to 4EBP-mediated inhibition and m7GTP-dependent translation, and iv) translation on bicistronic mRNA. The *GCH1*–3′ IRES-mediated translation is resistant to eIF4G cleavage and to mTORC1 inhibition and 4EBP-mediated inhibition. That *GCH1*–3′ IRES facilitates translation is evident with A-capped mRNA in bicistronic construction, suggesting that the *GCH1*–3′ UTR element has IRES activity (Figure 7). The eIF4F complex may bind to mRNA via a cap structure or the *GCH1*–3′ UTR element. Binding of the eIF4F complex to the cap structure initiates the conventional pathway of translation, with translation of upstream ORF initiated from the first AUG codon. The eIF4F complex may bind to the *GCH1*–3′ UTR element via the binding of eIF4G to the element in a manner independent of eIF4E and the cap structure. Conventional translation factors and the 43S ribosome complex are recruited, and 80S complex formation on the 3′UTR initiates translation of dORF. The binding of eIF4F to two sites may occur simultaneously or may be competitive.

Despite this heterogeneity of IRES elements required by the host to recruit ribosomal subunits, conserved motifs preserve sequences that affect RNA structure and RNA–protein interactions, which are significant for IRES-driven translation (43). However, RNA-binding proteins (RBPs) composed of ribonucleoprotein complexes are recruited by the short RNA motifs. IRES elements may consist of combinations of short modules, providing sites of inter-action for ribosome subunits, eIFs and RBPs, with implications for the definition of criteria to identify novel IRES-like elements throughout the genome (43). Our results strongly suggest that the *GCH1*–3′ UTR element constitutes a short motif that recruits eIF4G. Translational-enhancing elements, which facilitate translation through interactions with eIF4G positioned downstream of a reporter gene, can also enhance translation of the upstream gene in a cap-independent manner. The tethering of eIF4G on mRNA experiments demonstrated the effect of the distance between the cap structure and initiation codon on the translation efficiency of mRNAs. These findings support the RNA looping hypothesis that translational enhancement by eIF4G is recognition of the initiation codon by the ribosome bound to the ribosome-recruiting sites (45). The RNA looping model provides a logical explanation for the augmentation of translation by enhancing elements located upstream and/or downstream of a protein-coding region.

Recent genome-wide studies explored the effect of repression of the master regulator mTOR kinase on protein synthesis (50,51). mTOR inhibition led to dephosphorylation of eIF4E-binding protein (4E-BP), and disruption of interactions between eIF4E and eIF4G (50,51). Thus, translation of bulk mRNAs, even under harsh conditions, is not inhibited to the extent expected from the ratio of capped-to-uncapped mRNA translation efficiencies. The m7G cap is still utilized for translation initiation, but whether it uses residual amounts of active eIF4E or some other cap-binding protein(s) has not been determined. We found that 3′ IRES-mediated translation is resistant to the mTOR inhibitor Torin 1, indicating that translation of dORF occurs when inhibition of mTOR1 reduces eIF4E-mediated translation initiation. Further study will provide the fundamental mechanisms by which the cis-elements recruit eIF4G and function as IRES or CITE in the individual context, and the way in which they are involved in regulating the translation of cellular mRNA.

SUPPLEMENTARY DATA

ACKNOWLEDGEMENTS

FUNDING

REFERENCES

1. Hinnebusch,A.G. (2014) The scanning mechanism of eukaryotic translation initiation. *Annu. Rev. Biochem.*, **83**, 779–812.
2. Jackson,R.J. (2013) The current status of vertebrate cellular mRNA IRESs. *Cold Spring Harb. Perspect. Biol.*, **5**, a011569.
3. Walsh,D. and Mohr,I. (2011) Viral subversion of the host protein synthesis machinery. *Nat. Rev. Microbiol.*, **9**, 860–875.
4. Asnani,M., Kumar,P. and Hellen,C.U. (2015) Widespread distribution and structural diversity of Type IV IRESs in members of Picornaviridae. *Virology*, **478**, 61–74.
5. Wilson,J.E., Pestova,T.V., Hellen,C.U. and Sarnow,P. (2000) Initiation of protein synthesis from the A site of the ribosome. *Cell*, **102**, 511–520.
6. Yamamoto,H., Unbehaun,A. and Spahn,C.M.T. (2017) Ribosomal chamber music: toward an understanding of IRES mechanisms. *Trends Biochem. Sci.*, **42**, 655–668.
7. Jan,E., Mohr,I. and Walsh,D. (2016) A cap-to-tail guide to mRNA translation strategies in virus-infected cells. *Annu. Rev. Virol.*, **3**, 283–307.
8. Gradi,A., Svitkin,Y.V., Imataka,H. and Sonenberg,N. (1998) Proteolysis of human eukaryotic translation initiation factor eIF4GII, but not EIF4GI, coincides with the shutoff of host protein synthesis after poliovirus infection. *PNAS*, **95**, 11089–11094.
9. Belsham,G.J., McInerney,G.M. and Ross-Smith,N. (2000) Foot-and-mouth disease virus 3C protease induces cleavage of translation initiation factors eIF4A and eIF4G within infected cells. *J. Virol.*, **74**, 272–280.
10. Kobayashi,M., Arias,C., Garabedian,A., Palmenberg,A.C. and Mohr,I. (2012) Site-specific cleavage of the host poly(a) binding protein by the encephalomyocarditis virus 3c proteinase stimulates viral replication. *J. Virol.*, **86**, 10686–10694.
11. Svitkin,Y.V., Herdy,B., Costa-Mattioli,M., Gingras,A.C., Raught,B. and Sonenberg,N. (2005) Eukaryotic translation initiation factor 4E availability controls the switch between cap-dependent and internal ribosomal entry site-mediated translation. *Mol. Cell. Biol.*, **25**, 10556–10565.
12. Garrey,J.L., Lee,Y.Y., Au,H.H.T., Bushell,M. and Jan,E. (2010) Host and viral translational mechanisms during cricket paralysis virus infection. *J. Virol.*, **84**, 1124–1138.
13. Garaigorta,U. and Chisari,F.V. (2009) Hepatitis C virus blocks interferon effector function by inducing protein kinase R phosphorylation. *Cell Host Microbe*, **6**, 513–522.
14. Ali,I.K., McKendrick,L., Morley,S.J. and Jackson,R.J. (2001) Truncated initiation factor eIF4G lacking an eIF4E binding site can support capped mRNA translation. *EMBO J.*, **20**, 4233–4242.
15. Svitkin,Y.V., Gradi,A., Imataka,H., Morino,S. and Sonenberg,N. (1999) Eukaryotic initiation factor 4GII (eIF4GII), but not eIF4GI, cleavage correlates with inhibition of host cell protein synthesis after human rhinovirus infection. *J. Virol.*, **73**, 3467–3472.
16. Thompson,S.R., Gulyas,K.D. and Sarnow,P. (2001) Internal initiation in Saccharomyces cerevisiae mediated by an initiator tRNA/eIF2-independent internal ribosome entry site element. *PNAS*, **98**, 12972–12977.
17. Jang,S.K., Krausslich,H.G., Nicklin,M.J., Duke,G.M., Palmenberg,A.C. and Wimmer,E. (1988) A segment of the 5' nontranslated region of encephalomyocarditis virus RNA directs internal entry of ribosomes during in vitro translation. *J. Virol.*, **62**, 2636–2643.
18. Pestova,T.V., Shatsky,I.N., Fletcher,S.P., Jackson,R.J. and Hellen,C.U. (1998) A prokaryotic-like mode of cytoplasmic eukaryotic ribosome binding to the initiation codon during internal translation initiation of hepatitis C and classical swine fever virus RNAs. *Genes Dev.*, **12**, 67–83.
19. Tsukiyama-Kohara,K., Iizuka,N., Kohara,M. and Nomoto,A. (1992) Internal ribosome entry site within hepatitis C virus RNA. *J. Virol.*, **66**, 1476–1483.
20. Weingarten-Gabbay,S., Elias-Kirma,S., Nir,R., Gritsenko,A.A., Stern-Ginossar,N., Yakhini,Z., Weinberger,A. and Segal,E. (2016) Comparative genetics. Systematic discovery of cap-independent translation sequences in human and viral genomes. *Science*, **351**, aad4939.
21. Gilbert,W.V. (2010) Alternative ways to think about cellular internal ribosome entry. *J. Biol. Chem.*, **285**, 29033–29038.
22. Shatsky,I.N., Dmitriev,S.E., Andreev,D.E. and Terenin,I.M. (2014) Transcriptome-wide studies uncover the diversity of modes of mRNA recruitment to eukaryotic ribosomes. *Crit. Rev. Biochem. Mol. Biol.*, **49**, 164–177.
23. Hashimoto,S., Nobuta,R., Izawa,T. and Inada,T. (2019) Translation arrest as a protein quality control system for aberrant translation of the 3'-UTR in mammalian cells. *FEBS Lett.*, **593**, 777–787.
24. Hamby,S.E., Thomas,N.S., Cooper,D.N. and Chuzhanova,N. (2011) A meta-analysis of single base-pair substitutions in translational termination codons ('nonstop' mutations) that cause human inherited disease. *Hum. Genomics*, **5**, 241–264.
25. Skabkin,M.A., Skabkina,O.V., Hellen,C.U. and Pestova,T.V. (2013) Reinitiation and other unconventional posttermination events during eukaryotic translation. *Mol. Cell*, **51**, 249–264.
26. Powell,M.L., Leigh,K.E., Poyry,T.A., Jackson,R.J., Brown,T.D. and Brierley,I. (2011) Further characterisation of the translational termination-reinitiation signal of the influenza B virus segment 7 RNA. *PLoS One*, **6**, e16822.
27. Machida,K., Shigeta,T., Yamamoto,Y., Ito,T., Svitkin,Y., Sonenberg,N. and Imataka,H. (2018) Dynamic interaction of poly(A)-binding protein with the ribosome. *Sci. Rep.*, **8**, 17435.
28. Sizova,D.V., Kolupaeva,V.G., Pestova,T.V., Shatsky,I.N. and Hellen,C.U. (1998) Specific interaction of eukaryotic translation initiation factor 3 with the 5' nontranslated regions of hepatitis C virus and classical swine fever virus RNAs. *J. Virol.*, **72**, 4775–4782.
29. Kieft,J.S., Zhou,K., Jubin,R. and Doudna,J.A. (2001) Mechanism of ribosome recruitment by hepatitis C IRES RNA. *RNA*, **7**, 194–206.
30. Lytle,J.R., Wu,L. and Robertson,H.D. (2002) Domains on the hepatitis C virus internal ribosome entry site for 40s subunit binding. *RNA*, **8**, 1045–1055.
31. Lyons,A.J., Lytle,J.R., Gomez,J. and Robertson,H.D. (2001) Hepatitis C virus internal ribosome entry site RNA contains a tertiary structural element in a functional domain of stem-loop II. *Nucleic Acids Res.*, **29**, 2535–2541.
32. Filbin,M.E. and Kieft,J.S. (2011) HCV IRES domain IIb affects the configuration of coding RNA in the 40S subunit's decoding groove. *RNA*, **17**, 1258–1273.
33. Ostareck,D.H., Ostareck-Lederer,A., Shatsky,I.N. and Hentze,M.W. (2001) Lipoxygenase mRNA silencing in erythroid differentiation: The 3'UTR regulatory complex controls 60S ribosomal subunit joining. *Cell*, **104**, 281–290.
34. Kozak,M. (1998) Primer extension analysis of eukaryotic ribosome-mRNA complexes. *Nucleic Acids Res.*, **26**, 4853–4859.

35. Zinshteyn,B., Rojas-Duran,M.F. and Gilbert,W.V. (2017) Translation initiation factor eIF4G1 preferentially binds yeast transcript leaders containing conserved oligo-uridine motifs. *RNA*, **23**, 1365–1375.

36. Liu,Q., Kirubakaran,S., Hur,W., Niepel,M., Westover,K., Thoreen,C.C., Wang,J., Ni,J., Patricelli,M.P., Vogel,K. *et al.* (2012) Kinome-wide selectivity profiling of ATP-competitive mammalian target of rapamycin (mTOR) inhibitors and characterization of their binding kinetics. *J. Biol. Chem.*, **287**, 9742–9752.

37. Wolfson,R.L. and Sabatini,D.M. (2017) The dawn of the age of amino acid sensors for the mTORC1 pathway. *Cell Metab.*, **26**, 301–309.

38. Showkat,M., Beigh,M.A. and Andrabi,K.I. (2014) mTOR signaling in protein translation regulation: implications in cancer genesis and therapeutic interventions. *Mol. Biol. Int.*, **2014**, 686984.

39. Schenone,S., Brullo,C., Musumeci,F., Radi,M. and Botta,M. (2011) ATP-competitive inhibitors of mTOR: an update. *Curr. Med. Chem.*, **18**, 2995–3014.

40. Kleppe,A.S. and Bornberg-Bauer,E. (2018) Robustness by intrinsically disordered C-termini and translational readthrough. *Nucleic Acids Res.*, **46**, 10184–10194.

41. Young,D.J., Makeeva,D.S., Zhang,F., Anisimova,A.S., Stolboushkina,E.A., Ghobakhlou,F., Shatsky,I.N., Dmitriev,S.E., Hinnebusch,A.G. and Guydosh,N.R. (2018) Tma64/eIF2D, Tma20/MCT-1, and Tma22/DENR recycle Post-termination 40S subunits in vivo. *Mol. Cell*, **71**, 761–774.

42. Guydosh,N.R. and Green,R. (2014) Dom34 rescues ribosomes in 3' untranslated regions. *Cell*, **156**, 950–962.

43. Lozano,G., Francisco-Velilla,R. and Martinez-Salas,E. (2018) Deconstructing internal ribosome entry site elements: an update of structural motifs and functional divergences. *Open Biol.*, **8**, 108155.

44. Terenin,I.M., Smirnova,V.V., Andreev,D.E., Dmitriev,S.E. and Shatsky,I.N. (2017) A researcher's guide to the galaxy of IRESs. *Cell. Mol. Life Sci.*, **74**, 1431–1455.

45. Paek,K.Y., Hong,K.Y., Ryu,I., Park,S.M., Keum,S.J., Kwon,O.S. and Jang,S.K. (2015) Translation initiation mediated by RNA looping. *Proc. Natl. Acad. Sci. U.S.A.*, **112**, 1041–1046.

46. Kolupaeva,V.G., Pestova,T.V., Hellen,C.U. and Shatsky,I.N. (1998) Translation eukaryotic initiation factor 4G recognizes a specific structural element within the internal ribosome entry site of encephalomyocarditis virus RNA. *J. Biol. Chem.*, **273**, 18599–18604.

47. López de Quinto,S., Lafuente,E. and Martínez-Salas,E. (2001) IRES interaction with translation initiation factors: functional characterization of novel RNA contacts with eIF3, eIF4B, and eIF4GII. *RNA*, **7**, 1213–1226.

48. Imai,S., Kumar,P., Hellen,C.U., D'Souza,V.M. and Wagner,G. (2016) An accurately preorganized IRES RNA structure enables eIF4G capture for initiation of viral translation. *Nat. Struct. Mol. Biol.*, **23**, 859–864.

49. Simon,A.E. and Miller,W.A. (2013) 3' cap-independent translation enhancers of plant viruses. *Annu. Rev. Microbiol.*, **67**, 21–42.

50. Hsieh,A.C., Liu,Y., Edlind,M.P., Ingolia,N.T., Janes,M.R., Sher,A., Shi,E.Y., Stumpf,C.R., Christensen,C., Bonham,M.J. *et al.* (2012) The translational landscape of mTOR signalling steers cancer initiation and metastasis. *Nature*, **485**, 55–61.

51. Thoreen,C.C., Chantranupong,L., Keys,H.R., Wang,T., Gray,N.S. and Sabatini,D.M. (2012) A unifying model for mTORC1-mediated regulation of mRNA translation. *Nature*, **485**, 109–113.